

# APPLICATION OF DIAMOND-LIKE CARBON COATINGS TO ELASTOMERS FRICTIONAL SURFACES

L. Martínez<sup>a,\*</sup>, R. Nevshupa<sup>a,d</sup>, L. Álvarez<sup>a</sup>, Y. Huttel<sup>a</sup>, J. Méndez<sup>a</sup>, E. Román<sup>a</sup>, E. Mozas<sup>b</sup>, J.R. Valdés<sup>b</sup>,

M.A. Jimenez<sup>b</sup>, Y. Gachon<sup>c</sup>, C. Heau<sup>c</sup>, F. Faverjon<sup>c</sup>

<sup>a</sup> *Instituto de Ciencia de Materiales de Madrid (ICMM-CSIC), Cantoblanco, 28049 Madrid, Spain*

<sup>b</sup> *Instituto Tecnológico de Aragón, María de Luna 8, 50018 Zaragoza, Spain*

<sup>c</sup> *HEF R&D, ZI Sud Rue Benoit Fourneyron, F42166 Andrezieux Boutheon Cedex, France*

<sup>d</sup> *Bauman Moscow State Technical University, 2-Baumanskaia 5, 105005 Moscow, The Russian Federation*

\* Corresponding author. Tel.:+34913349000;fax:+34913720623. E-mail address: [lidia.martinez@icmm.csic.es](mailto:lidia.martinez@icmm.csic.es) (L.Martínez).

## ABSTRACT

Nitrile-butyl rubber-like materials were coated with amorphous hydrogenated diamond-like carbon (DLC) coatings in order to modify their surface and tribological properties. Measurements of water contact angle were performed by the sessile drop method and showed that the coated samples are more hydrophobic with water contact angles up to 116°. The surface free energy of the elastomers was calculated by the acid–base regression method considering polar and dispersive contributions and the results were correlated with changes in the surface chemistry measured by X-ray photoelectron spectroscopy. It has been found that the lower presence of oxygen functional groups on the elastomer surfaces led to lower surface free energies, even though the polar contribution was not predominant. We also found that the DLC coatings led to a significant decrease of the surface free energy (up to 16%) and that there is a good correlation between the surface free energy values and the corresponding water contact angle values. The coefficient of friction was also measured and presented a significant decrease after coating with DLC.

## 1. Introduction

Acrylonitrile–butadiene rubbers (NBR) and hydrogenated acrylonitrile–butadiene rubbers (HNBR) are widely used in the automotive industry, due to their moderate cost, excellent resistance to oils, fuels and greases, processability and very good resistance to swelling by aliphatic hydrocarbons [1]. One effective way to increase the life in service of machine elements is to apply a thin coating of amorphous diamond-like carbon (DLC). Such coatings presented excellent tribological properties as they increase the frictional and wear performance of machine elements [2]. These DLC coatings have been extensively/predominantly used over metals,

ceramics and other inorganic materials. Recently, Nakahigashi et al. [3] reported lower friction and wear when coating elastomers with elastic DLC. The idea of applying a hard DLC film on elastomer materials was considered at first with reluctance because it does not sound logical to apply a thin hard film on a deformable substrate without the occurrence of interfacial delamination. Once it was proved to be possible, there exists a wide field of application for coated elastomer components in mechanics and especially automotive industry. In this work, DLC coatings were applied over a series of elastomers of the same family (NBR) in order to study the variation of these frictional surface properties and consider further optimization of the films. Water contact angle (CA) measurements proportioned information about the hydrophobicity of the surface that is crucial for applications in various branches of industry [4]. A surface is considered to be hydrophobic when the water CA is over 90° [5]. CA is typically the property measured for the non-stick coatings to estimate their surface energy. In the present work, the obtained results on the water CA were compared with a detailed analysis of the surface free energy calculated by the acid–base regression method. In addition, the influence of the surface chemistry and morphology was studied by means of X-ray photoelectron spectroscopy (XPS) and atomic force microscopy (AFM). Finally, the effect of DLC coatings deposited on the elastomer and/or the counterbody on the tribological performance of the elastomers was studied by measuring the coefficient of friction (COF) and by evaluating the friction-related noise and wear.

## 2. Experimental details

### 2.1. Materials and treatments

A comparison of the performance of NBR 7201, NBR 9003, NBR 8003 and HNBR 8001 elastomers was carried out with and without DLC coatings deposited on their surface.

Deposition of DLC films was performed in a vacuum deposition unit equipped with radiofrequency (RF) biasing. The chamber was pumped down to  $3 \times 10^{-6}$  mbar residual pressure. The  $\text{Ar}^+$  plasma etching of the surface lasted for 1h; after that an organosilicon precursor was introduced in the plasma for 7 min. Afterwards, acetylene was introduced in the plasma for 3h. During coating deposition the bias voltage was reduced. As elastomer materials are really sensitive to temperature, parameters were optimized to keep the temperature of each step of the process below the maximal admissible temperature (120 °C). Depending on the bias, the maximal temperature ranged between 75 and 100 °C. Preliminary experiments were performed, where the process was interrupted after heating and etching. The samples were observed afterwards, and neither noticeable surface modification nor plasticizer exhaust was observed.

Optical observation of a film deposited on elastomer (Fig. 1) shows a regular crack network along the valleys of the surface. It is now admitted that the presence of these

crack networks is a positive thing as it allows flexibility of the coating when the substrate is bent without interfacial delamination [6]. The thickness of the DLC coating on the elastomer was measured by a Mahr stylus profilometer and the resulting thickness was 3 mm. The counterbody used for tribological tests was a brass alloy (EN12164 CW164N). The PECVD process was used for the deposition of DLC on the counterparts. After degreasing and cleaning in ultrasonic bath, samples were introduced in a vacuum chamber with a base pressure of  $2 \sim 10^{-4}$  mbar and heated at 150 °C for 2 h for outgassing. Subsequently, Ar was introduced (60 sccm) in the chamber for plasma etching of the surface during 45 min. A pulsed bias voltage was applied to ignite the plasma. Then an organosilicon precursor was introduced in the plasma for 1 h. Finally, acetylene was introduced in the plasma for 1 h.

## 22. *CA measurement and surface free energy calculation*

Static CA measurements were carried out at room temperature by the sessile drop method using water droplets of 4 ml. The surface energy evaluation system (SEE) [4] was used for the acquisition of the drop images and further analysis of the drop shape. The CA measurements were repeated several times on each sample and the obtained results were averaged in order to minimize the measurement uncertainty. The recorded pictures were analyzed manually by the user, providing full control of CA determination.

The surface free energy was calculated by the acid–base regression method [4] using the same SEE system. This method enables to determine the electron-donor and electron-acceptor components of the surface energy. The total free surface energy ( $g$ ) is the sum of non-polar Lifshitz–Van der Waals ( $\gamma^{LW}$ ) and polar acid–base ( $\gamma^{AB}$ ) components. This last  $g^{AB}$  component includes electron-acceptor ( $\gamma^+$ ) and electron-donor ( $\gamma^-$ ) components, which are not additive [7]:

Five liquids were used for this analysis: water, glycerol, ethylene glycol, formamide and diiodomethane, whose properties are detailed in Table 1.

## 23. *XPS measurements*

All the samples were characterized by XPS. The measurements were carried out in an ultra-high vacuum (UHV) chamber with a base pressure of  $1 \sim 10^{-10}$  mbar, using a Phoibos 100 ESCA/Auger spectrometer, with non-monochromatized  $MgK_{\alpha}$  (1253.6 eV) X-rays. Wide energy range scan spectra and narrow energy scan spectra were recorded. The wide scans provided complete information about all the elements present in the samples while the narrow scans provided more accurate chemical information on specific elements and chemical bonds. The narrow scan spectra were recorded with an analyser pass energy of 15 eV. The contribution of the  $MgK_{\alpha}$  satellite

lines was subtracted and the spectra were subjected to a Shirley background subtraction formalism [8]. The binding energy scale was calibrated with respect to the C 1s peak at 285 eV [9,10].

#### 24. *AFM measurements*

The surface morphology was examined using AFM in the dynamic mode in order to avoid stick–slip problems during the measurements. The tip used was a silicon polygon-based pyramid with a height of 10–15 nm and a typical tip radius of 07 nm. The analysis of the images was carried out with WSxM software [11].

#### 25. *Tribological tests*

Tribological tests were conducted on a Plint TE77 tribometer with reciprocating configuration [12], which includes a control unit incorporating COMPEND acquisition software. The tests were carried out at a temperature of 23±2 °C with a relative humidity between 55% and 70%. The system provides sequence control of load, frequency and temperature in addition to the data acquisition of measured parameters. Fig. 2 shows an image of the reciprocating test system of the TE 77 tribometer.

The rubber specimens were square plates of side 10 mm and thickness 2 mm, glued to the steel tooling using cyanoacrylate adhesive. The coated surfaces of the rubber were cleaned with a clean laboratory tissue and the uncoated ones were cleaned with acetone.

The reciprocating friction tests consisted of eight steps that combined different values of normal load and friction frequency, as specified in Table 2. Various combinations of coated and uncoated elastomers and brass counterbodies were studied. All the tests were performed at room temperature with a linear stroke of the reciprocating motion of 15 mm.

### 3. **Results**

#### 3.1. *CA measurements and surface free energy calculations*

Fig. 3 represents the comparison of the water CA values measured on each elastomer before and after coating with DLC. In all cases, an increase in the water CA was registered after DLC deposition. The NBR-coated elastomers had CA values above 100°, which represented an increase of at least a 10% of CA after the DLC coating. On the contrary, the HNBR 8001 is the only elastomer tested whose CA remained below 100° in particular and 84° after coating with DLC. For this elastomer only a small variation of the CA close to the experimental uncertainty was registered.

The crack network observed in the DLC surfaces (Fig. 1) can influence the final value of the CA measured. A higher surface roughness usually leads to lower CA. However, in our experiments the coatings with similar crack structure induced different modifications on the CA measured, depending on the substrate. The importance of the substrate on the

CA measured on the DLC-coated samples is especially evident from different behaviour observed on the hydrogenated HNBR in comparison to the NBRs. Furthermore, in the case of the HNBR, the variation in the CA after coating with DLC is within the experimental uncertainty and, therefore, this suggests that surface roughness is not a determinant factor in the final value measured.

Total surface free energy and its components were calculated using acid–base regression method and are shown on Table 3. For the three NBR elastomers, the total surface free energy decreased after the DLC coating, whereas the HNBR showed the opposite tendency. The dispersive component ( $\gamma^{LW}$ ) was the main contribution to the surface free energy. In the case of the NBR elastomers, both the polar and dispersive components of the surface free energy presented a tendency to decrease with the DLC coating that involved a decrease in the total surface free energy. Only in the case of NBR 8002, a small increase in  $\gamma^{LW}$  was measured. This tendency was also observed on the HNBR 8001, where  $\gamma^{LW}$  increased and  $\gamma^{AB}$  remained above 1 mJ/m<sup>2</sup>, mainly due to a high contribution of the electron-donor component ( $\gamma^-$ ).

### 3.2 Surface analysis

In Table 4 the chemical composition (%at) of the elastomer surfaces obtained from the wide energy range scan XPS spectra is compared for uncoated elastomers and after DLC coating. The main elements present on the samples before and after coating with DLC were carbon, oxygen and nitrogen. Small amounts of other elements have been found. Among these elements sulphur and zinc are typically used in curing processes of rubber [14]; silicon is also typically present on the elastomer, while the origin of tin, argon and chlorine is unclear. In the present analysis these elements were not taken into account as it was supposed that they have no real influence on the surface material properties [1]. An increase in the oxygen content was the only modification observed in the surface composition after adding the DLC coatings.

In order to investigate changes in the main bonding of the elastomers, the curve-fitting procedure of XPS spectra of the C 1s core level peaks was performed. The results of the curve fittings are illustrated in Fig. 4 and are summarized in Table 5. The four components used for the fitting are derived from the expected chemistry of the samples, taking into account the natural oxidation process of the elastomers. The main contribution to the carbon peak was fixed at 285 eV, which corresponds either to the C–C or the C–H bond [10]. The following components at higher binding energies correspond to oxidized components: C–O bonds at 286.3 eV, C=O at 288.1 eV and O–C=O at 289 eV [15].

The C=C bond was included in the C–C component as the gap between these binding energies is only 0.3 eV [7]. The C=N bond from the NBR structure was not considered due to the small contribution of nitrogen to the final composition. After these considerations, the variation of each contribution after the DLC coating was analysed keeping the binding

energy and the full- width at half-maximum (FWHM) of each untreated elastomers fixed.

The results evidenced a decrease in the C–C contribution corresponding to the backbone structure of the elastomers after coating with DLC, as a consequence of the formation of oxygen functional groups, mainly in the form of C–O, and also O–C=O. In the case of the C=O contribution, the changes observed were smaller than on the other oxygen-containing components. Among the tested samples, the HNBR elastomer presented the highest increase in O functional groups.

Variation of the surface morphology of the samples at nanoscale was studied by AFM. Fig. 5 presents as an example the surface of the NBR 7201 elastomer before (left) and after (right) DLC coating. It can be observed that the surface appearance of the elastomers is modified with the DLC coating. Among the several parameters that can be used to characterize the surface roughness, three different roughness parameters were measured in this work: the root mean square (RMS), the maximum height difference ( $R_{max}$ ) and the average roughness ( $R_a$ ). All of them revealed an increase in the surface roughness of the elastomers by a factor of four after the DLC coating. This was surprising since after DLC deposition a lower surface roughness was expected, as it usually occurs on metals [13]. However, over these elastomers, DLC coatings produced an increase in the surface roughness on nanoscale.

### 3.3 *Tribological tests*

The COF of the elastomers was measured along the eight steps specified in Table 2. Additionally, the loss of weight of the tested surfaces was measured after friction tests. Four different combinations of coated and uncoated specimens and counterbodies were studied for each elastomer. Fig. 6 illustrates the results of the friction tests, whereas Table 6 displays the obtained values.

It can be observed that for most elastomers DLC coating produced a significant decrease in the COF, in tests with both coated and uncoated counterparts. The NBR 8002 is the only elastomer that presented a significant decrease in the COF when the counterpart was not coated. When the friction tests were performed with uncoated elastomer and coated counterpart, there also appears a significant reduction in the COF, especially for NBR 8002 and HNBR 8001, but not as large as the reduction achieved by coating the elastomers.

When the elastomer is coated, there is a tendency to reduce friction noise. Nevertheless, this conclusion must be handled with care, since only the qualitative appearance of noise has been registered, and a detailed analysis of the magnitude and frequency of the noise has not been performed.

Finally, wear analysis failed to provide any conclusive evidence, since the weight losses during the friction test (25 min) were negligible with respect to the weight of the samples (around 11 g), and wear tracks were not observed.

#### 4. Discussion

In this work, the CA of water measured by the sessile drop method was used as a first approximation to estimate the surface free energy of DLC coatings on elastomers. The results obtained presented a good correlation between the CA measured and the surface free energy calculated by the acid–base regression method.

For NBR elastomers coated with DLC, the CA of water increased from 10% to 22%. These results clearly indicate the increase in the hydrophobic character of the elastomer surfaces. This finding is consistent with previous works, where an increase in the hydrophobic properties of the DLC-coated elastomers was explained by the presence of a mixture of  $sp^2$  and  $sp^3$  hybridized carbon bonds in the DLC coating. This response is usually related to a lower reactivity of the coated surface. Indeed, in our experiments we measured a decrease in the surface free energy of the NBR elastomers coated with DLC. Characterization of hydrophobicity of the elastomer surfaces by the measurement of the CA of water is a good method to determine the modifications on the polarity of the elastomer surfaces and the corresponding chemical activity after DLC coating [16].

For the hydrogenated HNBR elastomer, a different behaviour was observed. The variations in the CA measured were statistically insignificant. In addition, this is the only material tested whose surface free energy increased after coating with DLC. It is suggested that hydrogenation of unsaturated bonds to form HNBR

results in different reactivity of the elastomer towards the DLC coatings. Despite the fact that the same type of DLC coating was deposited on all the elastomers, the extent of the modifications was different depending on the substrate. This is clearly evident from the comparison of the CA and the surface free energy for coated NBR and HNBR elastomers.

In addition to the surface chemistry, the CA can be modified by changing the surface roughness. More specifically the increase in the roughness of hydrophobic surfaces may result in a drastic decrease of water CA [17]. However, in the calculation of the surface free energy we could not take into account this factor. Analysis of the surface morphology shows different patterns on micro and nanoscales. As shown in Fig. 1, on microscale the surface pattern is characterized by a net of cracks and peeled-off zones. This net of cracks with distance between them from 5 to 50  $\mu\text{m}$  can be formed as a consequence of the large difference in mechanical properties, i.e. elastic modulus and hardness, of the coating and the elastomer substrates. This distance is much larger than the size of the AFM images, but much smaller than the size of the water droplet. Although all coated surfaces have equivalent surface roughness, the effect of the roughness on the CA should be the same for all elastomers. Thus, the difference in CA measured for coated NBR and HNBR elastomers must be explained by different factors including surface and bulk chemistry of substrates.

The chemical surface analysis evidenced an increase in the polar oxygen functional

groups on the coated surfaces. The presence of these groups leads to stronger attraction of polar liquids like water to the surface [18]. Therefore, lower CAs and higher surface free energies are expected for surfaces containing more polar oxygen functional groups. On the other hand, these

groups are mainly responsible for the increase in the acid component ( $\gamma^-$ ) of  $\gamma^{AB}$ , while this component is not predominant in the surface free energy.

The small changes in the surface chemistry and surface free energy may lead to small changes in the surface shear stress, which, in turn, not only leads to direct changes on the friction coefficient, but also affects the tangential deformation of the underlying elastomer substrate. Indeed, this deformation controls the energy dissipation during the friction of elastomers by elastic hysteresis. The increase in the surface shear stress results in an increase of the dissipated energy in the volume and *vice versa*. Therefore, the effect of the initial small surface changes on the friction coefficient is significantly enhanced. In our case, the small decrease observed in the surface free energy may result in a decrease in the adhesive component of the friction coefficient. Also, the CA of water decreased, thus decreasing the capillary component of friction.

From the NBR family, the NBR 8002 presents some peculiarities. The untreated elastomer presents the highest  $\gamma^{AB}$  values to the surface free energy due to an important  $\gamma^-$  contribution. This material presented the highest increase in the water CA after coating with DLC. The difference in this sample could be explained on the light of its surface composition. It presented the largest amount of carbon before and after DLC coating, which represented a low contribution of polar groups and, consequently, this sample exhibited the highest hydrophobic properties before and after coating deposition. In particular, this elastomer also presented the most significant decrease in the COF, which can be due to a reduction of the adhesive component of friction.

## 5. Conclusions

It was demonstrated that coating NBR and HNBR elastomers with DLC is a good method to improve the performance of these materials. It produces an increase in hydrophobic properties, surface roughness at nanometer and micrometer scales and decrease in the COF. However, a strong influence of the substrate characteristics was found on the final properties of DLC coating. Despite the fact that a similar surface roughness at micro and nanoscale was found in all the samples, the final surface properties change depending on the elastomer substrate tested.

The measurement of water CA can be used as an efficient way of estimating the evolution of the surface free energy. A comparison between the CA and the surface free energy measured by the acid–base regression method reflects a good correlation between both parameters.



The hydrogenated HNBR elastomer presented a different behaviour from the non-hydrogenated elastomers (NBRs). A larger amount of oxygen functional groups on the surface of HNBR after DLC coating induced the lowest increase in hydrophobic properties. As a result, HNBR is the only material that showed an increased surface free energy upon DLC coating.

DLC coatings produce a significant decrease in the COF of the elastomers and reduce their friction noise.

### **Acknowledgements**

The authors acknowledge the financial support of the EU from the Sixth framework programme in the KRISTAL Project no. 515837-2. L. Martínez and Y. Huttel acknowledge the Spanish “Ministerio de Educación y Ciencia” for the “Juan de la Cierva” and “Ramón y Cajal” programmes, respectively. R. Nevshupa acknowledges the “Marie Curie” programme (MIF1-CT-2006-22067).

### **References**

- [1] Degrange JM, Thomine M, Kapsa Ph, Pelletier JM, Chazeau L, Vigier G, et al. *Wear* 2005;259:684–92.
- [2] Lindholm P, Björklund S, Svahn F. *Wear* 2006;261:107–11.
- [3] Nakahigashi T, Tanaka Y, Miyake K, Oohara H. *Tribol Int* 2004;37:907–12.
- [4] Navrátil Z, Bursikova V, Stáhel P, Sira M, Zverina P. *Czechoslovak J Phys* 2004;54(Suppl. C):C882–7.
- [5] Kiuru M, Alakoski E. *Mater Lett* 2004;58:2213–6.
- [6] Pei YT, Bui XL, Zhou XB, de Hosson JThM. *Surf Coat Technol* 2008;202:1869–75.
- [7] Dilsiz N, Wightman JP. *Colloids Surf A* 2000;164:325–36.
- [8] Shirley DA. *Phys Rev B* 1972;5:2709.
- [9] Beamson G, Briggs D. *High resolution XPS of organic polymers*. New York: Wiley; 1992.
- [10] Zhang S-W. *Tribology of elastomers*. Tribology and interface engineering series, no. 47. Amsterdam: Elsevier; 2004.
- [11] Horcas I, Fernández R, Gómez-Rodríguez JM, Colchero J, Gómez-Herrero J, Baró AM. *Rev Sci Instrum* 2007;78:013705.
- [12] Stachowiak GW, Batchelor AW. *Engineering tribology*. Amsterdam: Elsevier; 2005.
- [13] Qi Y, Konca E, Alpas AT. *Surf Sci* 2006;600:2955–65.
- [14] Mitra S, Ghanbari-Siahkali A, Kingshott P, Rehmeier HK, Abildgaard H, Almdal K. *Polym Degrad Stabil* 2006;91:69–80.
- [15] Swaraj S, Oran U, Lippitz A, Friedrich JF. *WES Unger Plasma Process Polym*

2005;2:572–80.

[16] Alisoy HZ, Baysar A, Alisoy GT. *Physica A* 2005;351:347–57.

[17] Wu Y, Inoue Y, Sugimura H, et al. *Thin Solid Films* 2002;407:45–9.

[18] Laoharojanaphand P, Lin Tj, Stoffer Jo. *J Appl Polym Sci* 1990;40:369–84.

## Tables

**Table 1**

Components of surface free energy (in mJ/m<sup>2</sup>) of reference liquids

Liquid	$g_{\text{tot}}$	$g^{\text{LW}}$	$g^{\text{AB}}$	$g^-$	$g^+$
Water	72.80	21.80	51.00	25.50	25.50
Glycerol	64.00	34.00	30.00	57.40	3.92
Ethylene glycol	48.00	29.00	19.00	30.10	3.00
Diiodomethane	50.80	50.80	0.00	0.00	0.00
Formamide	58.00	39.00	19.00	39.60	2.28

**Table 2**

Normal load, oscillating frequency and duration of the steps of reciprocating friction tests

		Test description					
Step		Normal force (N)	Pressure (MPa)	Oscillating frequency (Hz)	Max. linear velocity (mm/s)	Time (s)	Distance (mm)
No.	ID						
1	Running-in	10	0.1	2.15	101.3	300	9675
2	Test #1	10	0.1	0.125	5.89	120	225
3	Test #2	10	0.1	0.215	10.1	120	387
4	Test #3	10	0.1	2.15	101.3	120	3870
5	Test #4	10	0.1	0.215	10.1	120	387
6	Test #5	40	0.4	0.215	10.1	120	387
	Pause	0	0.1	0	0	60	0
7	Test #6	10	0.1	0.215	10.1	120	387
8	Final test	10	0.1	2.15	101.3	120	3870

**Table 3**

Surface free energy of the studied samples determined by the acid–base regression method

<i>NBR 7201</i>					
U	51.0	49.7	1.3	1.4	0.3
C	42.8	42.4	0.4	0.2	0.2
<i>NBR 9003</i>					
U	36.5	36.2	0.3	0.01	3.6
C	34.1	33.6	0.5	0.38	0.1
<i>NBR 8002</i>					
U	36.7	31.2	5.5	1.2	6.3
C	33.3	32.6	0.7	0.7	0.1
<i>HNBR 8001</i>					
U	38.0	35.8	2.2	0.3	4.5
C	41.2	39.5	1.7	0.3	2.4

<sup>a</sup> U—uncoated, C—coated with DLC.

**Table 4**  
Chemical composition of the samples tested (% at)

Sample <sup>a</sup>	Composition (%at)							
	C	O	N	Ar	Cl	Sn	Zn	Si
<i>NBR 7201</i>								
U	88.4	6.8	0.5	2.7	0.4	–	0.2	1
C	87.7	7.9	2.7	–	0.1	–	Traces	1.6
<i>NBR 9003</i>								
U	90.7	6.9	–	1.1	0.6	0.1	0.1	0.5
C	88.6	7.9	1.3	–	0.4	0.5	–	1.3
<i>NBR 8002</i>								
U	98.2	1	–	–	–	–	–	0.8
C	98.3	1.3	–	–	–	–	–	0.3
<i>HNBR 8001</i>								
U	91.7	4	3.6	–	–	–	–	0.7
C	89.1	6.5	3.5	–	–	–	–	0.9

<sup>a</sup> U—uncoated; C—coated with DLC.

**Table 5**  
Percentage of the C 1s peak area of XPS core level spectra of the NBR samples

Sample <sup>a</sup>	% C 1s core levels			
	C–C/C–H	C–O	C=O	O–C = O
<i>NBR 7201</i>				
U	98	0	0	2
C	95	3	1	1
<i>NBR 9003</i>				
U	90	6	1	3
C	88	9	1	2
<i>NBR 8002</i>				
U	97	3	0	0
C	93	7	0	0
<i>HNBR 8001</i>				
U	91	5	4	0
C	86	11	2	1

<sup>a</sup> U—uncoated, C—coated with DLC.

**Table 6**  
Coefficient of friction of the elastomers

Step	$p$ (MPa)	Coefficient of function			
		Combination elastomer/counterbody <sup>a</sup>			
		C/C	U/C	C/U	U/U
<i>NBR 7201</i>					
Running-in	0.1	1.07	4.34	0.99	6.0
Test #1	0.1	0.65	3.10	0.48	3.5
Test #2	0.1	0.84	3.83	0.69	4.9
Test #3	0.1	1.03	4.50	0.98	5.0
Test #4	0.1	0.87	4.32	0.67	4.7
Test #5	0.4	0.38	1.76	0.36	2.0
Test #6	0.1	0.73	4.30	0.72	5.0
Final test	0.1	0.94	4.60	1.05	4.6
Friction noise		—	+	—	+
Lost weight (mg)		0.1	0.6	0	0.7
<i>NBR 9003</i>					
Running-in	0.1	1.03	3.61	0.96	5.27
Test #1	0.1	0.72	3.29	0.61	3.54
Test #2	0.1	0.96	4.09	0.88	4.28
Test #3	0.1	1.37	3.57	1.01	4.69
Test #4	0.1	0.92	3.88	0.84	4.17
Test #5	0.4	0.38	1.59	0.38	1.74
Test #6	0.1	0.87	3.68	0.82	4.24
Final test	0.1	1.25	2.62	1.01	4.43
Friction noise		—	+	—	+
Lost weight (mg)		0	0.3	0.2	0.1
<i>NBR 8002</i>					
Running-in	0.1	1.31	2.86	0.56	4.41
Test #1	0.1	1.39	2.27	0.44	2.75
Test #2	0.1	1.52	2.63	0.52	3.08
Test #3	0.1	1.20	2.23	0.53	4.52
Test #4	0.1	1.23	2.12	0.50	3.13
Test #5	0.4	0.65	1.10	0.27	1.15
Test #6	0.1	1.15	2.23	0.52	3.14
Final test	0.1	0.99	2.23	0.49	4.63
Friction Noise		+	+	+	—
Lost weight (mg)		0.1	0.3	0.2	0.2
<i>HNBR 8001</i>					
Running-in	0.1	1.00	3.77	0.76	5.89
Test #1	0.1	0.45	3.05	0.38	3.50
Test #2	0.1	0.57	3.56	0.55	4.80
Test #3	0.1	0.88	3.36	0.78	5.88
Test #4	0.1	0.61	3.52	0.55	4.55
Test #5	0.4	0.30	1.40	0.23	1.83
Test #6	0.1	0.57	3.23	0.50	5.05
Final test	0.1	0.87	3.11	0.78	6.20
Friction noise		—	+	—	+
Lost weight (mg)		0.2	0.5	0	0.1

<sup>a</sup> C—coated, U—uncoated.

## Figures

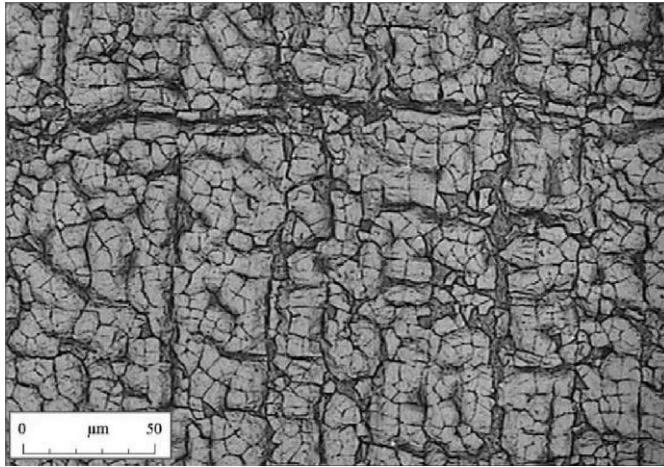


**Fig. 1.** Optical microphotograph of a DLC-coated elastomer surface.

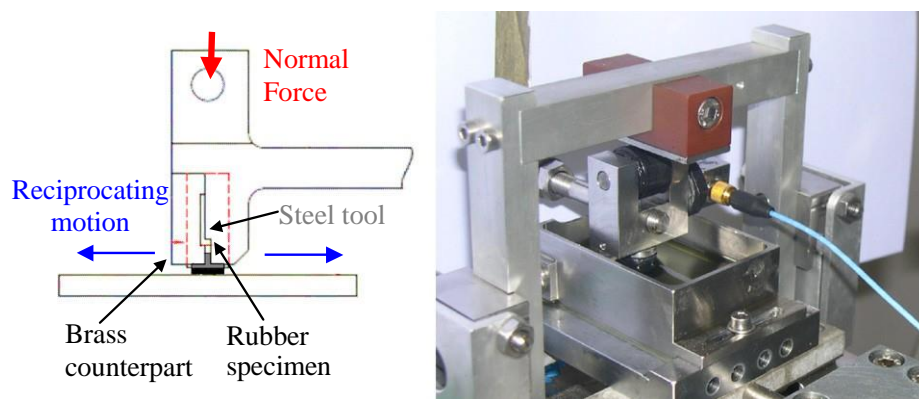


**Fig. 2.** General scheme of the reciprocating motion Plint TE77 tribometer.

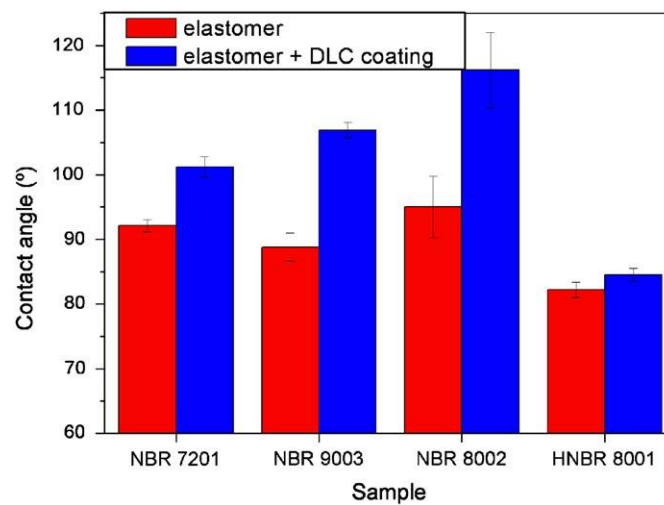


**Fig. 3.** Water CA measurements before and after coating with DLC.

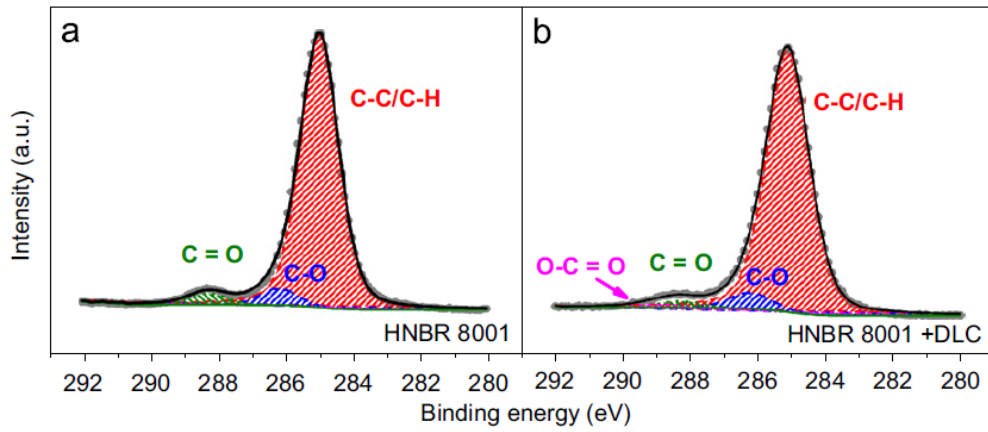


**Fig. 4.** C 1s core levels of the uncoated (a) and coated with DLC (b) HNBR.

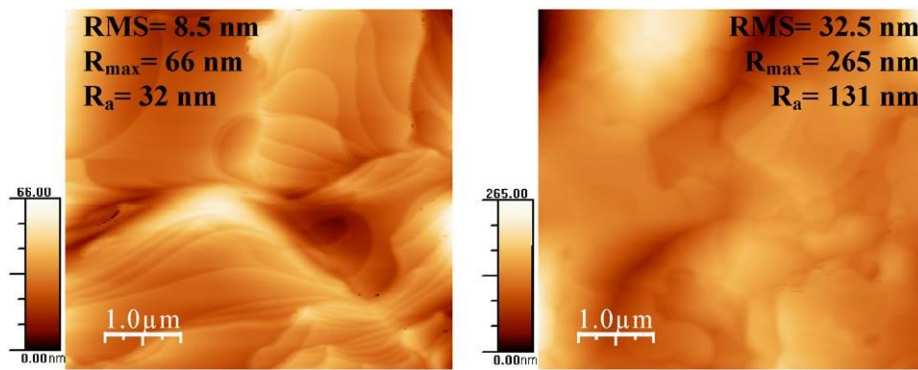


**Fig. 5.** AFM images of uncoated (left) and coated with DLC (right) NBR 7201 elastomer.

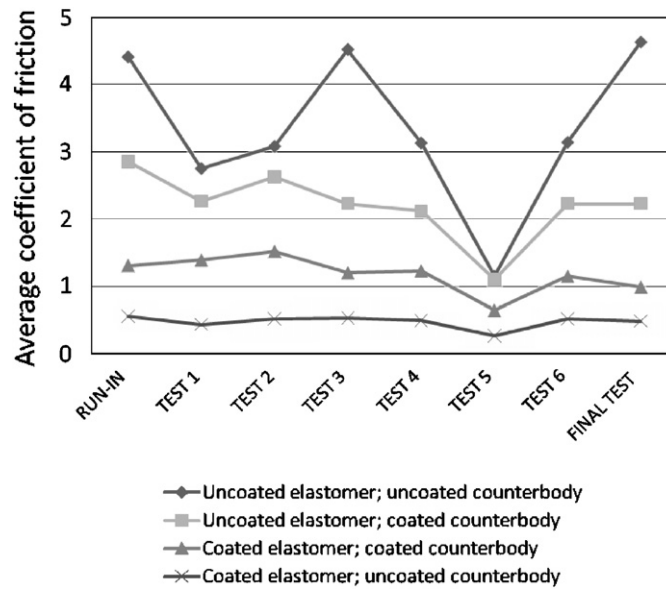


**Fig. 6.** Example of one of the friction tests performed on NBR 8002.